International Journal of Oral Science www.nature.com/ijos

ARTICLE OPEN

PPAR-γ activation promotes xenogenic bioroot regeneration by attenuating the xenograft induced-oxidative stress

Tingting Lan[1,2], Fei Bi[1], Yuchan Xu[1], Xiaoli Yin[3,4], Jie Chen[1], Xue Han[1] and Weihua Guo[1,5]✉

Xenogenic organ transplantation has been considered the most promising strategy in providing possible substitutes with the physiological function of the failing organs as well as solving the problem of insufficient donor sources. However, the xenograft, suffered from immune rejection and ischemia-reperfusion injury (IRI), causes massive reactive oxygen species (ROS) expression and the subsequent cell apoptosis, leading to the xenograft failure. Our previous study found a positive role of PPAR-γ in anti-inflammation through its immunomodulation effects, which inspires us to apply PPAR-γ agonist rosiglitazone (RSG) to address survival issue of xenograft with the potential to eliminate the excessive ROS. In this study, xenogenic bioroot was constructed by wrapping the dental follicle cells (DFC) with porcine extracellular matrix (pECM). The hydrogen peroxide (H_2O_2)-induced DFC was pretreated with RSG to observe its protection on the damaged biological function. Immunoflourescence staining and transmission electron microscope were used to detect the intracellular ROS level. SD rat orthotopic transplantation model and superoxide dismutase 1 (SOD1) knockout mice subcutaneous transplantation model were applied to explore the regenerative outcome of the xenograft. It showed that RSG pretreatment significantly reduced the adverse effects of H_2O_2 on DFC with decreased intracellular ROS expression and alleviated mitochondrial damage. In vivo results confirmed RSG administration substantially enhanced the host's antioxidant capacity with reduced osteoclasts formation and increased periodontal ligament-like tissue regeneration efficiency, maximumly maintaining the xenograft function. We considered that RSG preconditioning could preserve the biological properties of the transplanted stem cells under oxidative stress (OS) microenvironment and promote organ regeneration by attenuating the inflammatory reaction and OS injury.

International Journal of Oral Science (2023)15:10 ; https://doi.org/10.1038/s41368-023-00217-4

INTRODUCTION

Bioroot regeneration, characterized by ligament-to-bone attachment regeneration, has been considered as the most ideal regenerative way for tooth loss as its potential in recovering the normal sensation functions of natural tooth root. In previous studies, treated dentin matrix (TDM) based root/periodontal tissue engineering system has been successfully constructed with a great potential for periodontal ligaments (PDLs) regeneration.[1,2] However, in future clinical application, porcine derived ECM (TDM) will be the most widely used bio-scaffold to replace the failing organs and solve the problem of the limited donor source.[1,3] With the xenogenic TDM (xTDM)-based tissue engineered bioroots implanted, the heterologous antigens, which can not be completely removed by decellularization, will greatly aggravate the nonspecific inflammatory response and subsequent overproduction of ROS.[3,4]

Appropriate ROS concentration is vitally important in a variety of pathophysiological conditions by maintaining the microenvironment homeostasis through eliminating inflammatory mediums when injury occurs. Excessive intracellular ROS will amplify the inflammatory response,[5,6] which will induce genome instability with intracellular DNA damages through activating nuclear factor-kappa B (NF-κB) pathway in macrophages, promoting the macrophages polarizing to M1 phenotype,[7–9] directly causing the transplanted stem cells' death and multipotency impairment.[5,6,10,11] Moreover, abundant M1 polarized macrophages will increase the secretion of inflammatory factors, which could further recruit the neutrophils around the transplantation site and thus, aggravate inflammatory reaction.[12] In addition to the excessive ROS production, the decreased intracellular antioxidant capacity with down-regulated expression of SOD, glutathione peroxidase (GPx), and glutathione (GSH) also contributes to redox imbalance in the xenograft transplantation process,[13] making the tissue more vulnerable to OS and inflammatory reaction. The aggravated inflammation in the microenvironment could cause great damage to the cells, contributing to the xenograft failure.

Given the importance of OS and inflammatory response in the survival of the transplanted organ, it is of great importance to suppress ROS expression to alleviate the inflammation after the procedure of transplantation. It has been reported that when the excessive ROS is scavenged,[13] the regeneration process of the destroyed tissue in islet graft can be restarted to some extent. An emphasis on ROS control under the situation of promoting renal

[1]National Engineering Laboratory for Oral Regenerative Medicine & Engineering Research Center of Oral Translational Medicine, Ministry of Education & State Key Laboratory of Oral Diseases & National Clinical Research Center for Oral Diseases & Department of Pediatric Dentistry, West China School of Stomatology, Sichuan University, Chengdu, China; [2]School of Medicine, Nankai University, Tianjin, China; [3]Department of Pediatric Dentistry, Tianjin Stomatological Hospital, School of Medicine, Nankai University, Tianjin, China; [4]Tianjin Key Laboratory of Oral and Maxillofacial Function Reconstruction, Tianjin, China and [5]Yunnan Key Laboratory of Stomatology, The Affiliated Hospital of Stomatology, School of Stomatology, Kunming Medical University, Kunming, China
Correspondence: Weihua Guo (guoweihua943019@163.com)

Received: 17 September 2022 Revised: 11 January 2023 Accepted: 16 January 2023
Published online: 16 February 2023

transplantation survival has been widly proposed during last 20 years since the most serious complications in kidney transplantation often result from OS.[14–16] Similarly, during ECM-based bioroots transplantation process, the application of antioxidant N-Acetyl-L-cysteine (NAC) has obviously improved the PDLs regeneration efficiency by preserving the biological function of the transplanted stem cells, verifying the importance of antioxidation in bioroots transplantation.[17] In order to acquire an favorable outcome of xenogenic bioroots transplantation, not only controlling the overproduction ROS is essential, but enhancing the host's ability to defend against immune rejection is also an imperative requirement. Therefore, co-transplantation of xenogenic bioroots with a drug that could mediate the immune evasion as well as alleviate the OS damage is a promising strategy for xenogenic organ survival.

Peroxisome proliferator-activated receptor γ (PPARγ) receptor is an important signal molecule in regulating various physiological and pathological process-like inflammation, immune reaction and cell metabolism.[18–21] Recently, PPARγ agonist rosiglitazone (RSG) shows superiority on modulating immune microenvironment by promoting M2 macrophage polarization during acute immune rejection of the perioperative period of xenogenic organ transplantation.[3] Moreover, RSG also shows strengths in inflammation controlling and neuron preservating during renal transplantation,[22] making it a good candidate for microenvironment regulation of xenobiotic roots.

Our previous studies verified the efficiency of RSG on immunomodulation with the potential of alleviating the early stage immune rejection.[3] Therefore, in this study, we focused on exploring the protective effect of RSG on the intracellular environmental homeostasis of the transplanted stem cells, referring as DFCs in the xenogenic bioroots system under oxidative stress. We constructed an in vitro OS model with H_2O_2. SD rat orthotopic transplantation model was established to explore whether the antioxidant effect of RSG on the transplantation microenvironment could promote the final regeneration results of the xenogenic bioroots. For further verifying the role of RSG in tissue remodeling process under OS, xenogenic bioroot was cultured in subcutaneous areas of SOD1 knockout ($SOD1^{-/-}$) mice. We discovered a positive effect of RSG on suppressing ROS expression, resulting in a promotion on the implanted organ survival. This approach demonstrates a potential for xenogenic tissue or organ regeneration with PPARγ.

RESULTS

Special biological properties of pTDM and rDFC were conducive to construct xenogenic bioroots

Compared to porcine natural dentin matrix (pNDM), pTDM showed a porous and lax structure, through which proteins could be easily released (Fig. 1a). Large amounts of protein were continuously released into the culture supernatant in the first five days of pTDM culture and its concentration decreased significantly along incubation time (Fig. 1b). Additionally, a significant promotion effect on the cell's viability by pTDM protein, either in higher or lower concentration, was detected (Fig. 1c). In order to further confirm the kinds of proteins released from pTDM, ELISA assay was conducted. It showed a sustained release mode with a relative high concentration of the osteogenic or odontogenic differentiation-related proteins like Biglycan, bone glaprotein (BGP/OCN), TGF-β1, dentin matrix protein 1 (DMP-1) and dentin sialoph-osphoprotein (DSPP) within 4 weeks (Fig. 1d). Next, rDFC was harvested from the alveolar fossa of mandible and the characteristics of rDFC were explored. A large number of spindle shaped cells migrated from the harvested tissue could be seen (Fig. 1e, i). The morphology of rDFC shifted towards fuzziness when extracellular matrix membrane formed (Fig. 1e). IF staining with positive vimentin and negative CK14 confirmed that the harvested cells were dental follicle mesenchymal stem cells rather than epithelial cells (Fig. 1f). At last, multiple differentiation potential of rDFC was determined with a large number of mineralized nodules formation by Alizarin red staining (ARS) after culturing in the osteogenic induction medium for 21 days and positively stained with β III tubulin by IF staining after culturing in the neurogenic induction medium for 2 hours (Fig. 1g, h). Above results suggested that rDFC wrapped with pTDM was a feasible strategy for constructing the xenogenic bioengineered roots and highlighted that pTDM's sustained biological proteins releasing had made it an ideal bioscaffold for inducing the odontogenic differentiation of rDFC.

RSG reversed the biological characteristics of H_2O_2-induced damaged cells in the xenogenic bioroot system with PPAR-γ receptor activation

To determine the optimum inducing concentrations, CCK-8 test was conducted after rDFC was cultured with different concentrations of H_2O_2 or RSG. As shown in Fig. 2a, over 25 μmol·L^{-1} H_2O_2 could directly induce large amounts of cells death and furthermore, over 10 μmol·L^{-1} RSG could lead to obvious decreased cell survival as shown in Fig. 2b. Therefore, 25 μmol·L^{-1} H_2O_2 was selected as working concentration to induce cellular oxidative stress while 10 μmol·L^{-1} RSG was used to explore the effect of RSG on the H_2O_2-induced damaged cells. It showed that cell survival increased slightly from 83% to 94% with RSG pretreated the H_2O_2 induced cells (Fig. 2c). In addition to the promotion on the cells viability, RSG also showed an improvement on cell migration. As shown in Fig. 2d, compared to the H_2O_2-induced cells, RSG pretreated cells showed an enhancement on the cell's migration at 24 h and 48 h, indicating the protective role of RSG on the migration ability of cells exposed to the oxidative stress (Fig. 2d). In order to further explore the effect of RSG on the osteogenic/odontogenic differentiation potential of rDFC treated with H_2O_2, ARS staining and RT-PCR experiment were carried out. Results of RT-PCR showed that compared to the control group (rDFC), the osteogenic/odontogenic differentiation ability of cells treated with H_2O_2 was significantly impaired, accompanied by down-regulated expression of ALP and COL-1. However, administration with RSG could partially reverse the inhibitory effect of H_2O_2 on osteogenic differentiation of cells, preserving its biological function close to the normal cells (Fig. 2e). Similarly, the number of mineralized nodules stained by ARS in cells stimulated by H_2O_2 significantly decreased after culturing in the osteogenic inducing medium for 21 days while pretreatment with 10 μM RSG could partially block this effect (Fig. 2f). These results suggested that RSG could protect the biological characteristics of H_2O_2-induced damaged cells in the xenogenic bioroot system with PPAR-γ receptor activation.

RSG alleviated the intracellular oxidative stress status in vitro

For exploring the intracellular ROS level of rDFC, DCFH-DA, JC-1 staining and TEM observation were conducted. In DCFH-DA staining, there was an obvious elevated ROS expression of rDFC induced by H_2O_2 while an significant decreasing ROS expression of rDFC pretreated with 10 μmol·L^{-1} RSG, judged by fluorescence intensity and quantitative analysis (Fig. 3a, c). Consistent with this result, mitochondrial membrane potential detected by JC-1 staining also showed a relatively low mitochondrial membrane potential of rDFC induced by H_2O_2 while a higher level of mitochondrial membrane potential of rDFC with RSG pretreatment, judged by red fluorescence intensity, confirming the positive role of RSG in controlling ROS expression (Fig. 3b). For evaluating the antioxidant capacity of cells, total antioxidant capacity of rDFC stimulated with different chemical regents were determined. As shown in Fig. 3d, when treated with H_2O_2, the cells antioxidant capacity decreased significantly from 181 μmol·L^{-1}·g^{-1} to 135 μmol·L^{-1}·g^{-1} while it elevated to 216 μmol·L^{-1}·g^{-1} with RSG pretreating the H_2O_2-induced cells (Fig. 3d). TEM observation showed highly swollen mitochondria with mitochondrial membrane rupture, mitochondrial ridge continuity broken, even

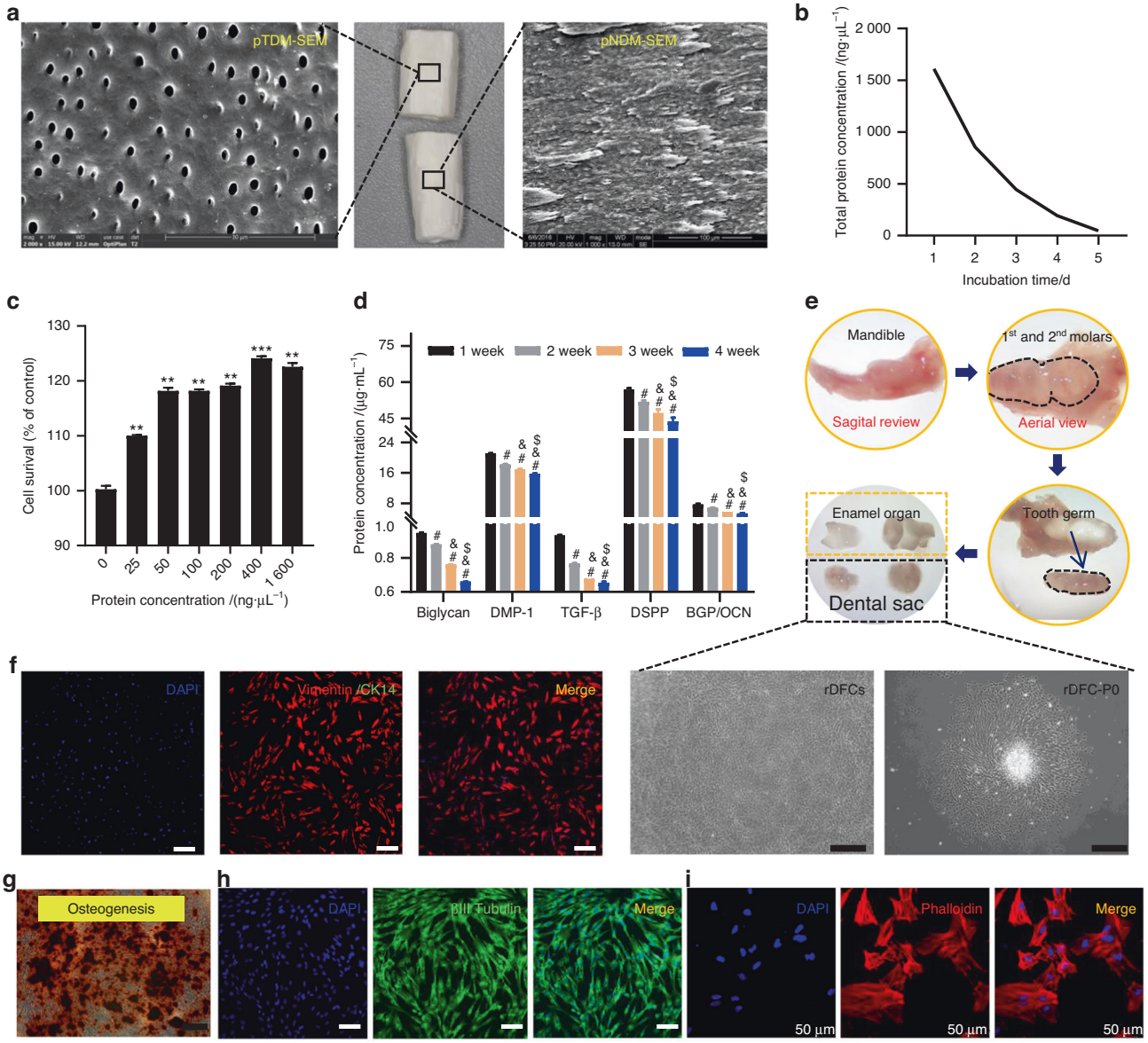

Fig. 1 Special characteristics of pTDM and rDFC were conducive to construct xenogenic bioroots. **a** SEM image of pTDM and pNDM. **b** Concentrations of the protein released from pTDM at different culture time points. **c** Effect of the different concentrations of pTDM protein on rDFC's viability. $^{**}P < 0.01$; $^{***}P < 0.001$. **d** Expressions of Biglycan, BGP/OCN, TGF-β1, DMP-1, and DSPP in the pTDM extracts tested by ELISA kits. $^{\#}P < 0.05$, vs 1 week; $^{\&}P < 0.05$, vs 2 week; $^{\$}P < 0.05$, vs 3 week. Not significant statistical analyses are not presented. **e** rDFC harvested process and morphology observation with light microscope. Scale bar = 500 μm. **f** IF staining with Vimentin and CK14 to determine the source of cells. Scale bar = 200 μm. **g** ARS staining of rDFC cultured in the osteogenic induction medium for 14 days. Scale bar = 500 μm. **h** IF staining with βIII-Tubulin of rDFC cultured in the neurogenic induction medium for 2 h. Scale bar = 100 μm. **i** IF staining with phalloidin of rDFC to determine cell morphology under laser confocal scanning microscope

disappear and peripheral condensation of chromatin of the rDFC with H_2O_2 treated. When pretreated with RSG, the ultrastructure of mitochondria of rDFC tended to be normal, verifying the protective role of RSG on mitochondria exposed to H_2O_2-induced OS (Fig. 3e). To verify the intracellular inflammatory level, IL-4 concentration was determined by elisa test. As shown in Fig. 3e, compared to the control group with 0.607 pg·mL^{-1}, IL-4 expression of the H_2O_2-induced cells decreased obviously while RSG pretreatment could promote its concentration to 0.321 pg·mL^{-1} (Fig. 3f and Fig. S1b).

RSG suppressed xenograft induced-oxidative stress and inflammation

To explore whether RSG could be effective for improving the microenvironment of xenografts by controlling ROS level, orthotopic implant model of SD rats was built by transplanting the xenogenic bioengineered tooth organs into the alveolar fossa (Fig. 4a). With the xenograft transplanted, obvious acute immune rejection could be detected in the first weeks to months, as has been demonstrated by our previous study and others; specifically, a variety of CD3+CD4+ T lymphocytes[23] and M1 macrophages[2] was recruited to the implantation sites from 1 week to 1 month after the xenogenic bioroots were implanted. Therefore, 1 week and 1 month post-implantation were selected to be the time points for observation in later experiment. In order to detect the lipid peroxidation level of the xenogenic grafts, HNEJ-2 (4-hydroxynonenal, a product of lipid peroxidation) expression around the transplanted xenogenic bioroots were explored. It showed a significant down-regulation in pTDM-rDFCs/RSG group at 1 week; however, at 1 month post-

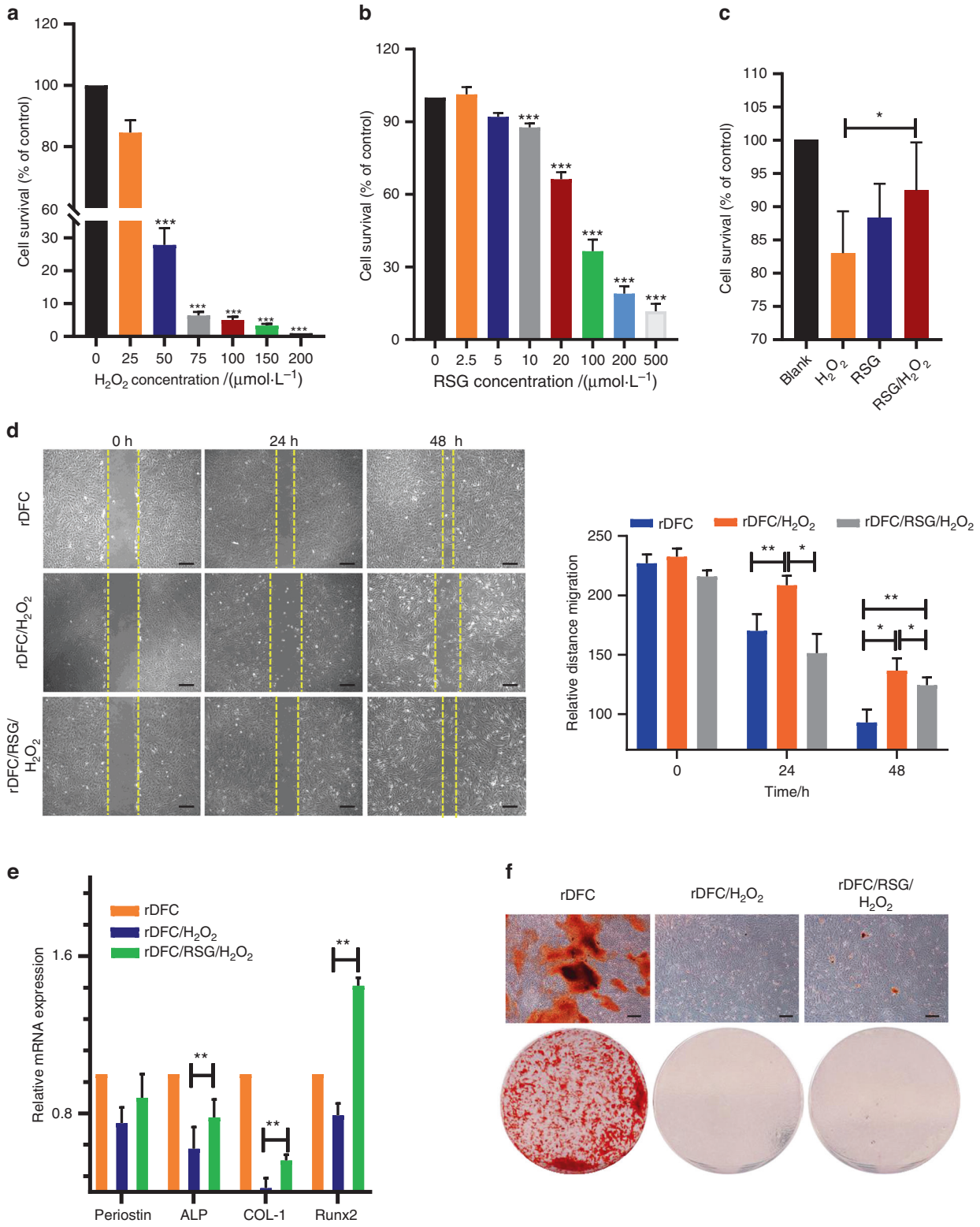

Fig. 2 RSG protected the biological characteristics of H_2O_2-induced damaged cells in the xenogenic bioroot system with PPAR-γ receptor activation. **a**, **b** Effects of different concentrations of H_2O_2 and RSG on cells viability. $^*P < 0.05$; $^{**}P < 0.01$; $^{***}P < 0.001$. **c** Effect of 10 μmol·L^{-1} RSG on the proliferation of 25 μmol·L^{-1} H_2O_2 induced-rDFC. **d** Migration efficiency of the rDFC under different stimulation at 0 h, 24 h, and 48 h. Scale bar = 500 μm. Not significant statistical analyses are not presented. **e** Relative mRNA expression of Periostin, ALP, COL-1 and Runx2 at 7 days. $^{**}P < 0.01$; Not significant statistical analyses are not presented. **f** Effect of RSG on the osteogenic differentiation potential of the H_2O_2-induced rDFC as determined by the amount of the mineralized nodules through ARS staining. Scale bar = 500 μm

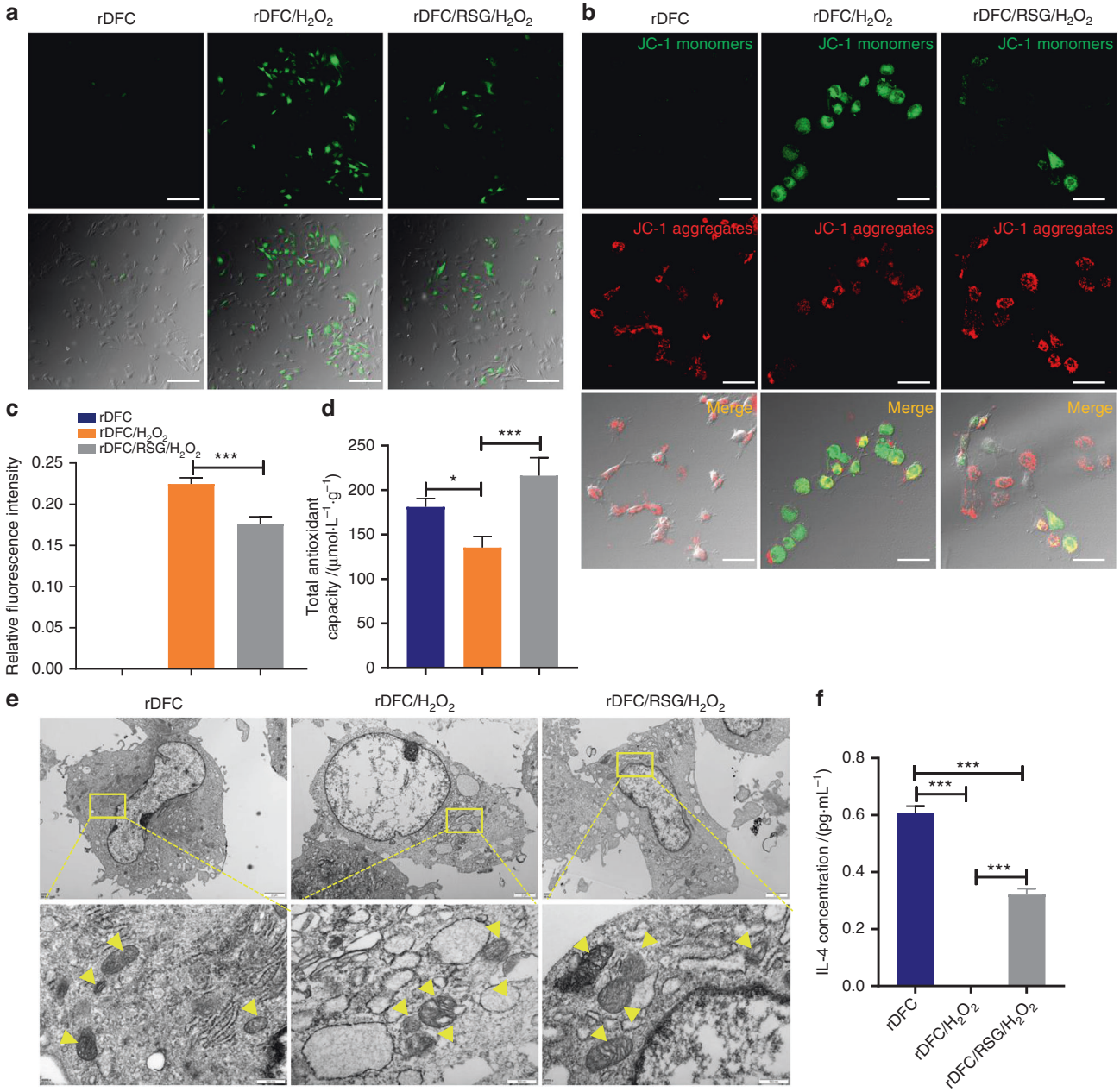

Fig. 3 RSG alleviated the intracellular oxidative stress status in vitro. **a** Intracellular oxidative stress detected by DCFH-DA. Scale bar = 100 μm. **b** Intracellular oxidative stress detected by JC-1. Scale bar = 50 μm. **c** relative fluorescence intensity in (a). ***$P < 0.001$. **d** Total antioxidant capacity of rDFC stimulated with different chemical regents. *$P < 0.05$; ***$P < 0.001$; Not significant statistical analyses are not presented. **e** Ultrastructure of mitochondria observed by TEM. Yellow arrow: mitochondria. **f** IL-4 concentration in the cell supernatant detected by ELISA test. ***$P < 0.001$

surgery, both of the groups with or without RSG treatment exhibited a lower HNEJ-2 level (Fig. 4b, d, e), indicating the effective role of RSG in suppressing the OS injury in the early stage post-transplantation. Consistent with this result, compared to pTDM-rDFCs group, expression of TNF-α in pTDM-rDFCs/RSG group showed an obvious decrease at 1 week while no difference at 1 month (Fig. 4c, f, g). Furthermore, relative to pTDM-rDFCs, TGF-β1 level in pTDM-rDFCs/RSG group showed a significant up-regulation at 1 week post-surgery while no difference at 1 month, indicating a promotion effect of RSG in the regeneration process of ECM-based bioroots. (Fig. 4h–k). Expressions of NOS2 and IL-1β around the xenograft were also explored at 1 week post-surgery (Fig. S1a).

RSG inhibited osteoclasts differentiation while promoted PDL-like tissue regeneration in xenogeneic bioroots remodeling process by suppressing oxidative stress

For detecting the antioxidant effect of RSG on the regeneration results, IF staining with SOD1, histological staining and trap staining of the samples were performed. It showed a significant decreased expression of SOD1 without RSG treatment at 1 week post-implantation while no difference at 1 month (Fig. 5a–d), which accorded with the results in Fig. 4b, f. At 2 months after implantation, it showed an active bone remodeling response in xenogenic bioroots system, including obvious bone adhesion and bone absorption, with large amounts of osteoclasts differentiation around pTDM. Consequently, no obvious collagen fibers

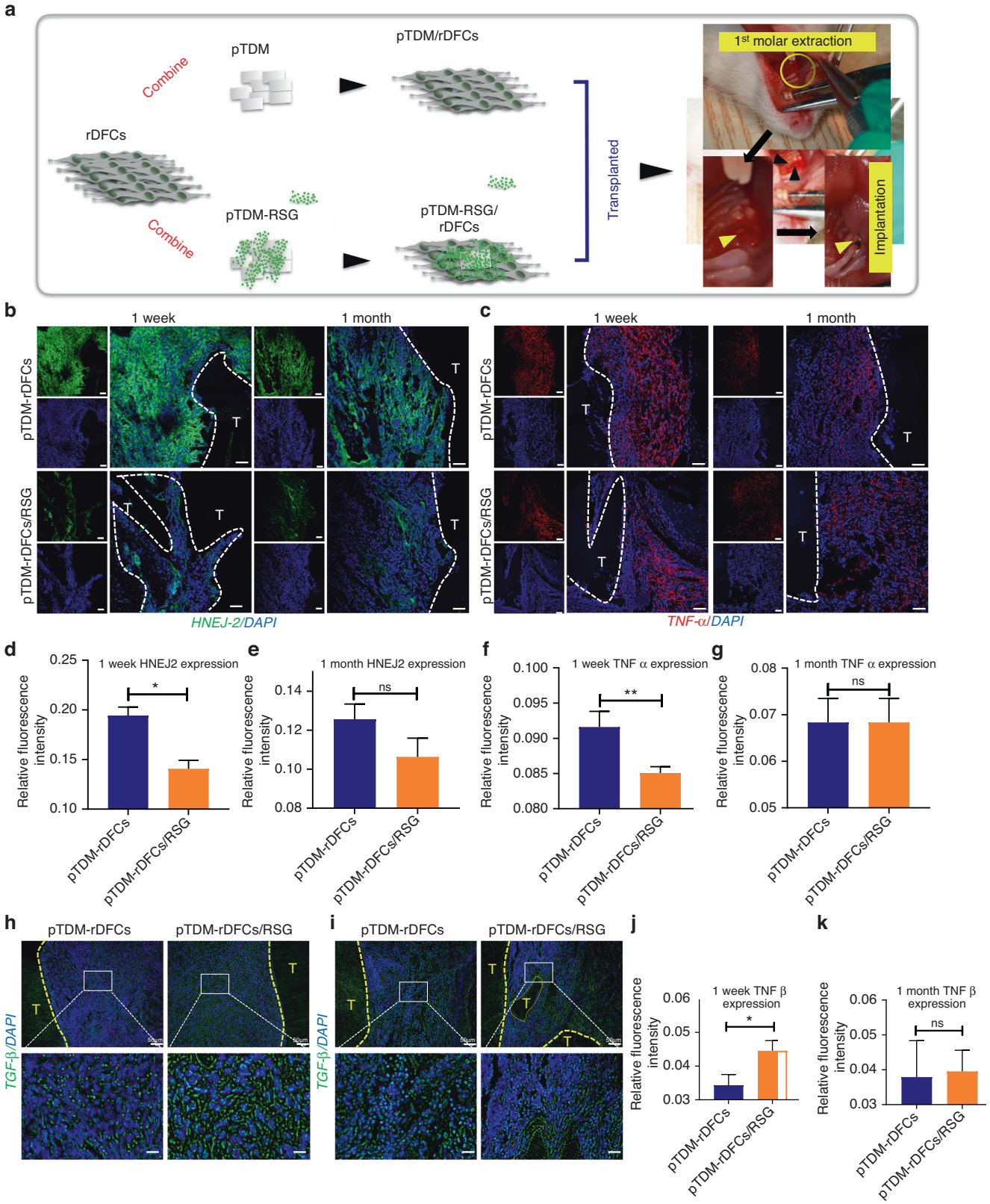

Fig. 4 RSG suppressed xenograft induced-inflammation. **a** Schematic illustration of orthotopic transplantation of SD rats. **b**, **c** IF staining of HNEJ-2 and TNF α around the xenogenic bioroots at 1 week and 1 month post-surgery. Scale bar = 20 μm; T: pTDM. **d**–**g** Relative quantitative analysis of HNEJ-2 and TNF α expressions in b and c for determining ROS level. *$P < 0.05$; **$P < 0.01$; ns: no significant statistical difference. **h** IF staining of TGF-β around the xenogenic bioroots at 1 week and 1 month (**i**) post-surgery. Scale bar = 20 μm. T: pTDM. **j**, **k** Relative quantitative analysis of TGF-β expressions in (**h**, **i**). *$P < 0.05$; ns, no significant statistical difference

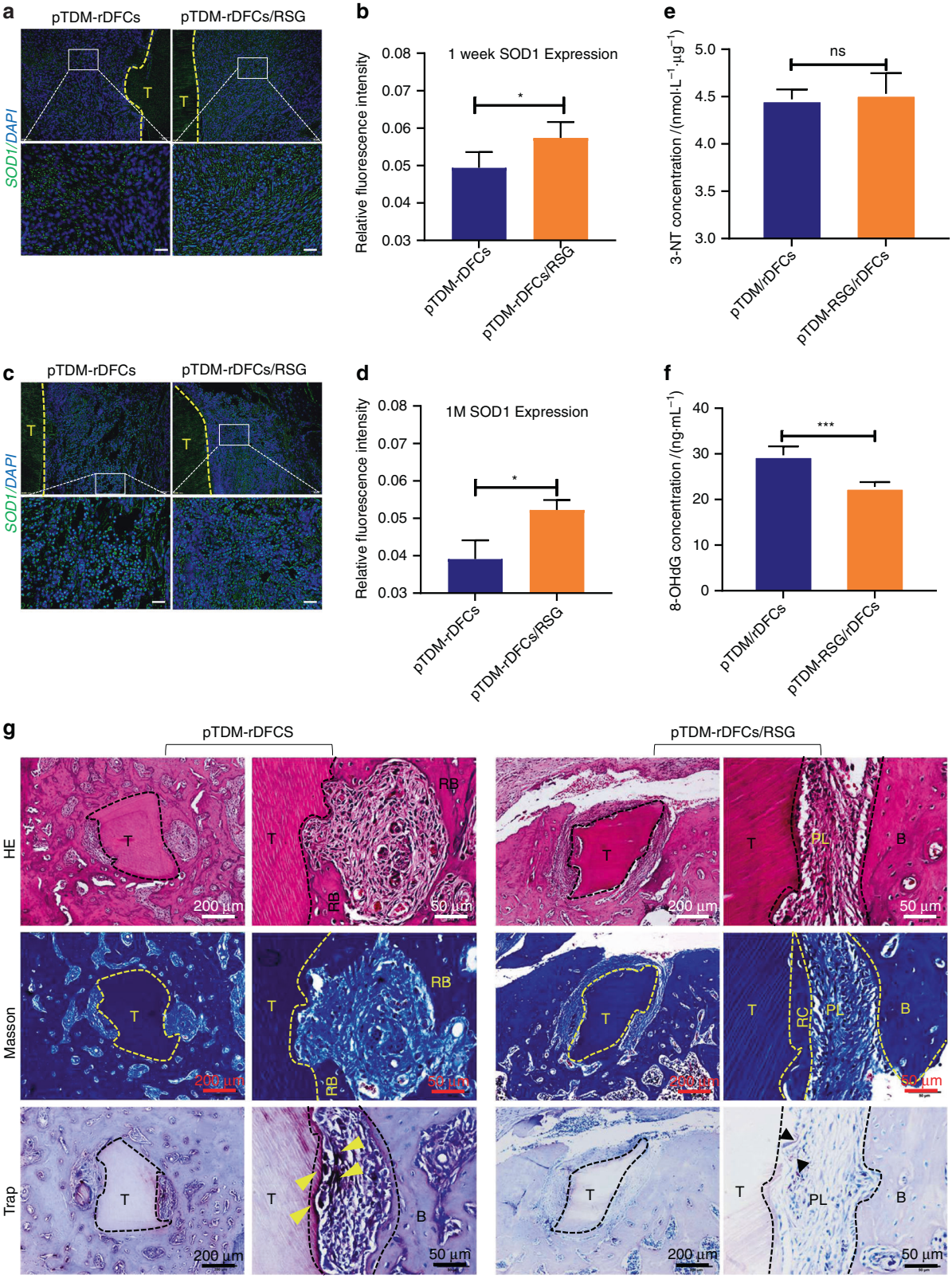

Fig. 5 RSG inhibited osteoclasts differentiation while promoted PDL-like tissue regeneration in xenogeneic bioroots remodeling process by suppressing oxidative stress. **a** IF staining of SOD1 (green) around pTDM at 1 week and 1 month (**c**) to detect the antioxidation ability of the host. T: pTDM. Scale bar = 20 μm. **b**, **d** Relative quantitative analysis of SOD1 expressions in (**a**, **c**). *$P < 0.05$. **e**, **f** Expressions of 3-NT and 8-OHdG around the xenogenic bioroots in vitro tested by Elisa. ns: no significant difference; ***$P < 0.001$; ns no significant statistical difference. **g** H&E, Masson and trap staining of the xenogeneic bioroots in alveolar fossa of rats at 2 months post-implantation. T, TDM; B, bone; RB, regenerated bone; RC, regenerated cementum; PL, periodontal-like tissues; OC (yellow and black arrows)

regeneration was observed. However, with RSG treatment, lots of collagen fibers, arranged perpendicular to pTDM surface similar to natural PDL, were regenerated without obvious bone adhesion or pTDM resorption. Besides, less osteoclasts were detected around pTDM (Fig. 5g). These results suggested that RSG could significantly inhibit osteoclasts formation but promote PDL-like tissue differentiation in xenogenic bioroots.

RSG prevented xenogeneic bioroots resorption under an OS injury microenvironment

To further confirm the mechanism of the promotion effect of RSG on PDL-like tissue regeneration, xenogenic bioroots treated with or without RSG were subcutaneously implanted into the back of $SOD1^{-/-}$ C57 mice (Fig. 6a). Two months after implantation, an obvious collagen matrix dissolution of pTDM accompanied by a low collagen fiber regeneration efficacy, a decreased periostin level and an elevated TNF-α expression were detected in xenogenic bioroots implanted in $SOD1^{-/-}$ C57 mice. On the contrary, when administrated with RSG, the transplanted pTDM maintained structural integrity without any collagen matrix dissolution or resorption. Other than that, large amounts of collagen fibers arranged perpendicular to pTDM were regenerated as shown in orthotopic implant model, demonstrating the importance of RSG in controlling ROS for enthesis regeneration in xenogenic bioroots (Fig. 6b, c). Compared to the general view in $SOD1^{-/-}$ C57 mice with RSG treatment, the transplanted xenogenic bioroots without RSG treatment showed less collagen fiber encapsulation and less newly regenerated angiogenesis on the surface of pTDM (Fig. 6c).

DISCUSSION

Dental follicle stem cells are a kind of adult stem cells with multidirectional differentiation potential to become osteoblasts, adipoblasts and neuroblasts,[24] which can be easily obtained from the third molar germs from adult subjects for the natural and normal development of teeth. Under an appropriate odontogenic induction environment, DFC is of great possibility to differentiate into periodontal ligament like tissues.[24] pTDM, similar to the human derived TDM (hTDM), characterized by lax and porous structure on its surface,[25] will be the main source of biological scaffold to provide structural strength to transplant DFC for constructing xenogenic bioroots, considering its superiority in continuous release of the odontogenic differentiation-related proteins like DMP-1/DSPP.[26] DMP-1/DSPP is considered to be an important protein in odontogenesis, which regulates cell mineralization.[1,27] When DMP-1/DSPP was knocked out, an obvious defect was observed on the surface of dental crown with dentin hypoplasia and tooth surface depression.[28] Therefore, pTDM can be served as an ideal biological inducing material for guiding the odontogenic differentiation of DFC, suggesting the potential of constructing xenogenic bioroots by DFC wrapped with pTDM. However, with the xenogenic TDM (pTDM) based bioroot implanted, acute immune rejection could be found both in vitro and in vivo with more CD3 + CD4 + T lymphocytes recruitment, Th1-related cytokines released increase and M1 macrophages polarization promotion,[3,23] which will cause excessive ROS production, leading to a series of pathological changes to the xenograft system.

OS can cause significant oxidative damage on DNA, protein and lipid, directly causing tissue pathological changes. Therefore, ROS level can be evaluated by measuring the level of free radical metabolites and the antioxidant enzymes. 8-OHdG is a product of DNA oxidative damage and is often used as a marker for detecting ROS level and DNA mutation for early diseases diagnosis.[29] Clinical studies have shown that 8-OHdG can be used as an important oxidative marker for evaluating the ROS level to confirm the effect of antioxidant therapy on colorectal cancer or cardiovascular diseases,[29,30] suggesting the probability of 8-OHdG in evaluating ROS expression. 3-NT is a kind of oxidation protein products originated from Tyrosine (Tyr) by adding a nitro group (-NO) with nitrating agents and is considered to be a marker of the formation of reactive nitrogens (RNs) in vivo. Nitrosative stress is closely related to oxidative stress. On the one hand, under oxidative stress, ROS can combine with RNs to form strong oxidant and nitrating agent to react with nucleic acids, proteins or other biological macromolecules. On the other hand, the oxidation product of nitrite-NO, also can damage intracellular bio-proteins, leading to the pathological changes.[31] At present, it has been reported that 3-NT can be used as an important marker of nitrosative stress to evaluate the therapeutic effect of antioxidants on asthma-chronic obstructive pulmonary disease overlap.[32] Therefore, in this study, 3-NT and 8-OHdG are both used to evaluate the ROS level.

PPARγ receptor exists in the nucleus of various cells and plays an important role in multiple physiological and pathological processes.[33,34] When activated, the microenvironment can be well regulated with an up-regulated expression of M2 macrophage polarization and a down-regulated level of inflammation, maintaining the immunity homeostasis.[35] However, when PPARγ receptor was knocked out, the immunomodulation effect of macrophage was deprived with obvious proinflammatory factors production.[36] Therefore, thanks to its superiority in immune regulation, PPARγ receptor agonist RSG has a wide application in xenotransplantation.[3,27] Consistent with this, in our study, RSG exhibited an anti-inflammatory effect on the H_2O_2 induced OS cells with decreased TNF-α expression but increased IL-4 concentration. Moreover, RSG also showed a positive role in scavenging ROS with increased cellular antioxidant capacity and a relative normal ultrastructure and mitochondrial membrane potential of mitochondria, suggesting the antioxidant capacity of RSG in the xenogenic bioroots system. In line with our study, previous research found that RSG could suppress the IRI during liver transplantation by promoting SOD1 expression.[1] Besides, previous study also demonstrated that RSG showed an antioxidant effects on a various of chronic diseases associated with oxidative stress, such as Alzheimer's syndrome, Parkinson's syndrome and diabetes mellitus. Systemic assessment showed an obvious decrease in ROS concentration of these diseases in the serum after RSG treatment,[37–39] verifying the importance of RSG in inhibiting the excessive ROS production. Most studies on how PPARγ regulated inflammation or IRI are focused on the pathway of nuclear factor κB (NF-κB). As one of the most important downstream proteins of PPAR-γ, NF-κB was demonstrated as a significant target in modulating ROS production and inflammation reaction.[40,41] It found that with the Thiazolidinediones (TZDs) administrated, transcription of NF-κB can be largely suppressed and thus, restraining the inflammatory signaling pathway activation.[35,41] Similarly, in this study, NF-κB also showed an obvious decrease expression with the RSG treated in the xenogenic bioroots system.

The features of the local immunological microenvironment largely determine the final regeneration results of the transplanted organs.[42] Consistent redox imbalance can remarkably contribute to internal environment dysfunction along with exaggeration of inflammation, the leading cause of graft failure.[43] During renal replacement therapy, OS-induced damage often caused the development of chronic kidney disease (CKD)-related systemic complications with the transplanted renal fibrosis even death.[44] However, when the OS was suppressed with decreased ROS concentration by ozone, damages to renal were obviously slighter, promoting the transplanted renal survival.[45] Similarly, in the heart transplantation, OS-derived damage contributes to progressive endothelial damage in the coronary arteries, leading to cardiac allograft vasculopathy initiation and progression,[46] greatly affecting the tissue remodeling process and function.[47]

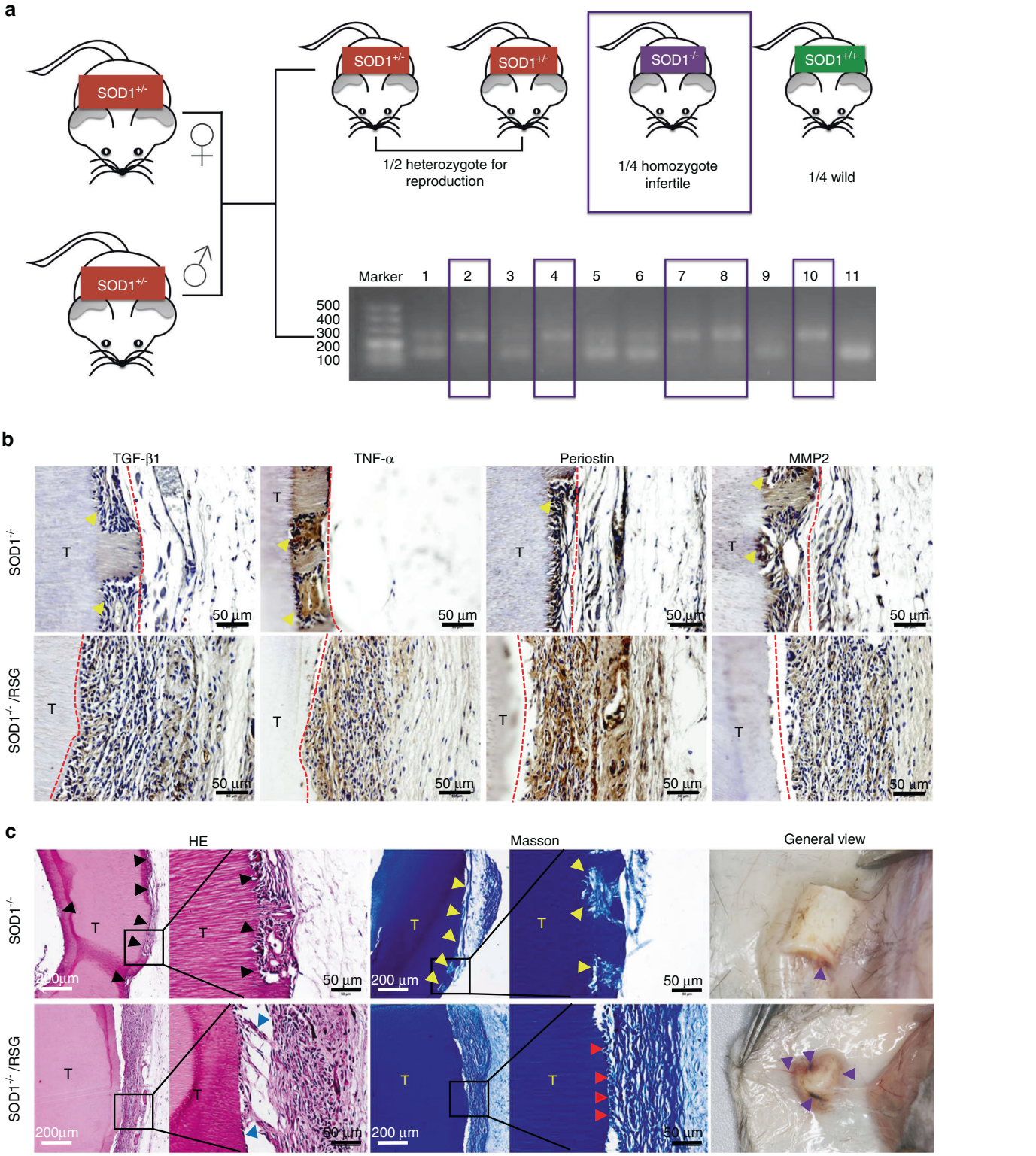

Fig. 6 RSG prevented xenogeneic bioroots resorption under an OS injury microenvironment. **a** clean homozygote SOD1 knockout mouse was defined by agarose gel electrophoresis. DNA marker (DL500) was made as the reference for DNA molecular weight; DNA bands between 100 and 200 bp was defined as SOD1 wt genotype mice (sample 9 and 11), 200–300 bp was defined as SOD1 KO genotype mice (sample 2, 4, 7, 8, and10), 100–200 bp and 200–300 bp coexistence was defined as heterozygous mice (sample 1,3,5, and 6). **b** IHC staining of the xenogeneic bioroots subcutaneously transplanted on the back of SOD1$^{-/-}$ C57 mice. T: TDM. **c** H&E, Masson staining and general view of the xenogeneic bioroots subcutaneously transplanted on the back of SOD1$^{-/-}$ C57 mice. T TDM; dissolved pTDM (black and yellow arrows); regenerated enthesis (red arrows); regenerated blood vessels (purple arrows)

Recently, our study verified an increased regeneration efficiency of the allogenic bioroots with ROS controlling through administrating with NAC.[2] Therefore, antioxidant therapy should be a significant component of the patients with organ transplantation.[48] Consistent with these studies, in this study, we also found an obvious up-regulated concentration of ROS after xenogenic bioroots implanted, resulting in a poor regeneration outcome accompanied by large amounts of bone adhesion and osteoclasts formation. However, when the intracellular ROS level and the inflammation expression in the transplantation microenvironment were well controlled by RSG, the organ survival rate was promoted significantly.

SOD1, as a subtype of the superoxide dismutases (SODs) with a surprisingly high cellular concentration,[49] can preserve the ROS concentration at a normal level together with the other two antioxidant enzymes GSH/GPX by forming an antioxidant enzyme system. Previous researches found that SOD1 knockout mice exhibited excessive ROS accumulation and defects on multiple system, resulting in dysplasia or sickness.[50–53] Recently, our previous study have just found an obvious ROS aggregation in $SOD1^{-/-}$ mice model with significant effects on mandible development. With the $SOD1^{-/-}$ mice growing up, ROS concentration peaked at 6 months with an obvious up-regulated H_2O_2 expression and decreased bone formation rate,[15] reminding us that 6 months years old $SOD1^{-/-}$ mice can be optimal for contributing OS model, with a potential to affect the tissue development and regeneration process. Therefore, for further detecting the antioxidant effect of RSG on xenogenic bioroots regeneration process, subcutaneous transplantation model was established in 4-month-old $SOD1^{-/-}$ mice and the observation time was extended to 2 months. Consistent with the results got in orthotopic transplantation model of SD rats and the findings in other organs transplantation,[22] RSG treatment was effective in promoting organ regeneration under OS microenvironment with less pTDM collagen decomposition and inflammatory factors secretion but more periostin expression, verifying the antioxidant role of RSG.

Despite of the positive role of RSG in promoting xenogenic bioroot regeneration through its antioxidant effect has been explored, the mechanism existed in this process needs to be further studied; moreover, big animal orthotopic transplantation models like dog, pig or monkey are also additionally required to verify the this active effect.

CONCLUSIONS

PPARγ agonist RSG can significantly alleviate the transplanted xenografts-derived OS damage by maintaining intracellular/immunity homeostasis, greatly promoting the regeneration outcomes and preserving the organs' function.

MATERIALS AND METHODS

Study approval

All animal experiments and procedures in this study were in accordance with institutional guidelines on animal welfare and were approved by the Institutional Laboratory Animal Care and Use Committee of Sichuan University (permit no. WCHSIRB-D-2019-063).

pTDM preparation

Xenogeneic teeth, harvested from the freshly extracted deciduous incisor teeth of porcine, were made into pTDM (porcine derived treated dentin matrix) following gradient demineralization by 17%, 10% and 5% ethylene diamine tetraacetic acid (EDTA, Sigma-Aldrich, St. Louis, MO, USA) as previously reported.[2] For pNDM (porcine derived natural dentin matrix), no demineralization was proceeded. All the obtained xECM were prepared for later experiment after performing ethylene oxide disinfection following freeze-dried for 8 h.

Biophysical properties of pTDM

SEM was used to determine the surface morphology of pTDM or pNDM at 15 kV. pTDM extracts were collected at different times after culturing in the saline with the weight/volume ratio of pTDM to solvent 1:5 (g: mL) for protein release detection. At each time-point, equal volume of fresh saline were added into the dishes after the extracts were totally taken away.

Cell culture and identification

rDFC (rat derived DFC) was isolated from the mandibular 1st molar of 3-5 days old SD rats and cultured in a complete α-MEM medium containing 10% FBS (HyClone) and 1% of 100 U of penicillin and 100 $\mu g \cdot mL^{-1}$ streptomycin at 37 °C with 5% CO_2 incubator. rDFC of 2-5 passage were seeded on 12-well plates at the number of 1×10^4 for following experiments. For rDFC sheets formation, 50 $mg \cdot mL^{-1}$ ascorbic acid was extra added into the medium to promote more extracellular matrix secretion when rDFC reached 70% confluence. For osteogenesis, 5 $mmol \cdot L^{-1}$ L-glycerophosphate (Sigma-Aldrich), 100 $nmol \cdot L^{-1}$ dexamethasone (Sigma-Aldrich), and 50 $mmol \cdot L^{-1}$ ascorbic acid were supplemented into the medium for 21 days' culturing. Subsequently, alizarin red S (ARS) staining was carried out after the cells were fixed with 4% paraformaldehyde (PFA). For neurogenesis, 2%DMSO (Amresco), 200 $\mu mol \cdot L^{-1}$ Butylated hydroxyanisole (Sigma-Aldrich), 25 $mmol \cdot L^{-1}$ KCl(bdhg.company, China), 2 $mmol \cdot L^{-1}$ Valporic acid sodium salt (Sigma-Aldrich), 10 $mmol \cdot L^{-1}$ forskolin (Sigma-Aldrich), 1 $mmol \cdot L^{-1}$ hydrocortisone(aladdin), and 5 $\mu g \cdot mL^{-1}$ insulin (Novo Nordisk) were additionally imparted for culturing 2 hours. Afterwards, IF staining with βIII Tubulin (abcam, ab78078) was performed. Briefly, cells were fixed with 4% PFA at room temperature for 15 minutes after washing with PBS for three times, then permeabilized with 0.25% Triton-X and blocked with 5% BSA. Primary antibody against βIII Tubulin at a dilution of 1:100 was added onto the fixed cells and incubated overnight at 4 °C. DAPI was used to stain nuclei finally. All the IF staining in this study were all in accordance with this procedure (primary antibodies: anti-Vimentin (santa cruz, sc-6260), anti-CK14 (millipore, MAB3232), anti-Alex Fluor 555 Phalloidin (CST,#8953)).

Cell proliferation, grouping and migration

CCK-8 test was carried out to assess the cells' proliferation. Different concentrations of H_2O_2 and RSG were separately added into the 96-well plates to culture the cells with the counting number of 4 000 per well initially. To detect the protection effect of RSG on the H_2O_2-induced damaged cells, rDFC was pretreated with 10 $\mu mol \cdot L^{-1}$ RSG for 4 h before 25 $\mu mol \cdot L^{-1}$ H_2O_2 was supplemented into the medium. With another 24 h culture, 10% (v/v) CCK-8 medium was added into each wells to culture the cells for 1.5 h at 37 °C for detecting the cell viability under different induced conditions. Cell viability was calculated based on the optical density (OD) value measured at 450 nm by absorbance microplate reader following the formula: (OD value in control - OD value in blank) / (OD value in experiment - OD value in blank). Cell migration was assessed through scratch test when the cells were fusion with different chemical regents stimulation. For cell grouping, rDFC in rDFC/H_2O_2 group was treated with 25 $\mu mol \cdot L^{-1}$ H_2O_2 for 24 hours while cells in rDFC/RSG/H_2O_2 group was pretreated with 10 $\mu mol \cdot L^{-1}$ RSG for 4 hours before cultured with 25 $\mu mol \cdot L^{-1}$ H_2O_2. Pipette tip was used to make a scrape on the monolayer cell and the non-adherent cells were removed from the plates with PBS washed for three times. The cell morphology was recorded under light microscopy (Nikon, Japan) at 0 h, 24 h, and 48 h for cell proliferation and migration evaluation.

ARS staining, RT-PCR and Western Blot

For evaluating the mineral nodule formation, ARS staining was performed after the cells were fixed with 4% PFA with culturing in the osteogenic medium for 21 days. After being cultured in the osteogenic medium for 7 days, rDFC was collected for assessing

the expressions of the osteogenic and odontogenic differentiation-related genes or proteins as previously described.[2] Briefly, real-time PCR was conducted by mixing the cDNA, which was at the final concentration of 100 ng·μL^{-1}, with SYBR Premix Ex Taq II (Tli RNaseH Plus) and primers (synthesized by Sangon Biotech) under the procedure of denaturing at 105 °C for 5 minutes followed by 40 cycles of PCR (95 °C for 30 s, 60 °C for 30 s, and 72 °C for 45 s). Relative expression levels were calculated using the $2^{-\Delta\Delta CT}$ method and normalized to the internal control GAPDH gene. The specific primer information was shown as follows (5′-3′): GAPDH (Forward: TATGACTCTACCCACGGCAAG; Reverse: TACTCAGCACC AGCATCACC); COL-1 (Forward: TGCTGCCTTTTCTGTTCCTT; Reverse: AAGGTGCTGGGTAGGGAAGT); Runx2 (Forward: TCATTTGCACTG GGTCACAT; Reverse: TCTCAGCCATGTTTGTGCTC); ALP (Forward:CGTTGACTGTGGTTACTGCTGA; Reverse: CTTCTTGTCCGTGTC GCTCAC); Periostin (Forward:TTCGTTCGTGGCAGCACCTTC; Reverse: TCGCCTTCAATGTGGATCTTCGTC); IL-1β (Forward:GGGATGATGAC-GACCTGCTA; Reverse: TGTCGTTGCTTGTCTCTCCT); TGF-β (Forward:-GACCGCAACAACGCAATCTATGAC; Reverse: CTGGCACTGCTTCCCG AATGTC); TNF-α (Forward:GCACGGAAAGCATGATCCGA; Reverse: AAGAGGCTGAGGCACAGACA); PPARγ (Forward:GCCCTTTGGTGAC TTTATGGAG; Reverse:GCAGCAGGTTGTCTTGGATGT). For western blot (WB) analysis, proteins were transformed into 0.22 μm polyvinylidene fluoride (PVDF) membranes, blocked with 5% skim milk at room temperature for 2 hours and then incubated with the primary antibodies of anti-IL-1β (Abcam, ab9787) and anti-NF-κB (CST, #8242) at a dilution ratio of 1:1 000 and anti-β actin (HUABIO, EM21002) at a dilution ratio of 1:5 000 at 4 °C overnight. WB signals were normalized to the internal control β-actin

Intracelluar ROS detection

For detecting intracelluar ROS level and inflammation expression, 2′, 7′ - dichlorofluorescein diacetate (DCFH-DA, Sigma, America) staining, JC-1 (Beyotime, China) staining, transmission electron microscope (TEM) test and Elisa assay were conducted as previously described.[2] In brief, cells were stained with JC-I or 10 μmol·L^{-1} DCFH-DA in dark at 37°C for 20 minutes for confocal microscope observation. For TEM detection, cells were fixed with 0.5% glutaraldehyde, dehydrated in gradient alcohol and permeated and embedded with resin. Consecutive 60-um-thick horizontal sections were obtained and double stained with uranium acetate and lead nitrate for 15 min for ultrastructural observation of mitochondria. Cell supernatants were collected for elisa test.

Animal models and surgery

pTDM/rDFCs group and pTDM-RSG/rDFCs group were included in animal experiments. pTDM was cultured in 200 ng·μL^{-1} RSG solution at 37°C with 5% CO_2 for 2 days and wrapped with the 5 ng·μL^{-1} RSG pretreated rDFCs, composed of pTDM-RSG/rDFCs group.

Transplant the xenogeneic bioroots into an orthotopic implant model of SD rats

pTDM was prepared into a uniform size of 1 mm × 1 mm × 2 mm for orthotopic implant after ethylene oxide disinfection. A total of 48 Sprague-Dawley rats (8 weeks old, females, 230–260 g), purchased from Chengdu Dossy Biological Technology Company, were performed surgery. After anesthetization with 2% pentobarbital sodium (3 mL·kg^{-1}) and Zoletil 50 (50 mg·kg^{-1}), skin, muscles and mucous membrane were blunt separated from the corner of the mouth until the bilateral 1st molars could be directly seen. The xenogeneic bioroots, pretreated with or without RSG, were transplanted into the mesiobuccal roots of the freshly extracted 1st molars. Then, the buccal and palatal mucosa were sutured to ensure that the implanted site could be completely covered. The muscle and skin in the open wounds were subsequently sutured in layers with 6–0 silk. At last, rats were injected with penicillin (1 U per 200 g) and fasted for 10 h post-surgery. 3–5 rats in each group were randomly selected and sacrificed at 1 week, 1 month and 2 months post-implantation. Maxilla, including the first molar extraction socket, was harvested and fixed in 4% PFA at 4°overnight, and then demineralized with 10% EDTA for 2 months. Paraffin sections and frozen sections were prepared for subsequent HE, Masson, trap staining and IF staining as previously described.[2] Briefly, frozen sections were washed by PBS for 3 times, repaired with antigen repair solution for 10 min, penetrated with 0.25% triton-100 for 10 minutes, blocked with 5% BSA for 1 h, separately incubated with the primary antibody anti-4 Hydroxynonenal (abcam, ab48506) and anti-TNFα(santa cruz, sc-52746) at a dilution of 1:200 overnight at 4°C, subsequently cultured with the corresponding second fluorescent antibody for 1 h, and finally stained with DAPI.

Tissue homogenates extraction

This experiment was carried out as previously described.[2] Briefly, SD rats were sacrificed at 7 days post-surgery under general anesthesia and subsequently, maxilla was separated; then, the transplantation along with the surrounding fibrous tissues were obtained for further experiments. Precooled normal saline was used to rinse the samples for removing the red blood cells as much as possible. After, the 1:100 diluted PMSF was mixed with the tissue at the volume ratio of 9:1 to grind into tissue homogenate. Supernatants of the specimens were collected by centrifugation at 12 000 r·min^{-1} for 15 min at 4 °C for subsequent Elisa analysis (8-OHdG/3-NT Elisa kit, Deco, Cat. #3455/ 3305).

Transplant the xenogeneic bioroots into a subcutaneous implant model of SOD1$^{-/-}$ C57 mice

pTDM was shaped into a hollow circular column (3 mm × 2 mm × 4 mm) for subcutaneous implant after ethylene oxide disinfection. Shanghai Model Organisms Center, Inc. was entrusted to establish an animal disease model of B6;129S-Sod1^{tm1Leb}J (SOD1$^{-/-}$) of C57 mice. After anesthetized with isoflurane, the prepared xenogeneic bioroots with or without RSG pretreated were implanted subcutaneously on the back of 4-month-old SOD1$^{-/-}$ C57 mice. The mice were killed 2 months after implantation and the samples were fixed at 4°C in 4% PFA overnight, and then demineralized with 10% EDTA for 4 months. Paraffin sections were prepared for subsequent histological staining as previously described.[2] Anti-TGFβ1 (abcam, ab92486), anti-Periostin (H-300) (santa cruz, sc-67233) and anti-MMP2 (abcam, ab92536) primary antibodies were applied at a dilution of 1:200.

Statistical analysis

All data are presented as the mean ± standard deviation (M ± SD). The Student's *t* test was used to assess differences between two groups. One-way analysis of variance (ANOVA) was performed to evaluate the discrepancies among multiple groups. All in vitro or in vivo work was represented at least three biological replicates by independent experiments.

DATA AVAILABILITY

All data associated with this study are presented in the paper.

ACKNOWLEDGEMENTS

This work was supported by the Nature Science Foundation of China (31971281, 32201073, 82270958), Innovative Talents Program of Sichuan Province (2022JDRC0043), Research and Develop Program, West China Hospital of Stomatology Sichuan University (RD-03-202106).

AUTHOR CONTRIBUTIONS

(I) Conception and design: Tingting Lan; (II) Administrative support: Weihua Guo; (III) Provision of study materials: Jie Chen, Xiaoli Yin; (IV) Collection and assembly of data: Xue Han, Yuchan Xu, and Xiaoli Yin; (V) Data analysis and interpretation: Fei Bi, Tingting Lan, and Weihua Guo; (VI) Manuscript writing: All authors; (VII) Final approval of manuscript: All authors.

ADDITIONAL INFORMATION

Supplementary information The online version contains supplementary material available at https://doi.org/10.1038/s41368-023-00217-4.

Competing interests: The authors declare no competing interests.

REFERENCES

1. Chen, J. et al. Treated dentin matrix-based scaffolds carrying TGF-β1/BMP4 for functional bio-root regeneration. *Appl. Mater. Today* **20**, 100742 (2020).
2. Zhang, J. et al. Improvement of ECM-based bioroot regeneration via N-acetylcysteine-induced antioxidative effects. *Stem. Cell. Res. Ther.* **12**, 202 (2021).
3. Lan, T. et al. Xenoextracellular matrix-rosiglitazone complex-mediated immune macrophage polarization. *Biomaterials* **276**, 121066 (2021).
4. Choi, H. J. et al. Blockade of CD40-CD154 costimulatory pathway promotes long-term survival of full-thickness porcine corneal grafts in nonhuman primates: clinically applicable xenocorneal transplantation. *Am. J. Transpl.* **15**, 628–641 (2015).
5. Maccarrone, M. & Brüne, B. Redox regulation in acute and chronic inflammation. *Cell. Death. Differ.* **16**, 1184–1186 (2009).
6. Lei, Y. et al. Redox regulation of inflammation: old elements, a new story. *Med. Res. Rev.* **35**, 306–340 (2015).
7. Seebach, E. & Kubatzky, K. F. Chronic implant-related bone infections-can immune modulation be a therapeutic strategy? *Front. Immunol.* **10**, 1724 (2019).
8. Vallée, A. & Lecarpentier, Y. Crosstalk between peroxisome proliferator-activated receptor gamma and the canonical WNT/β-Catenin pathway in chronic inflammation and oxidative stress during carcinogenesis. *Front. Immunol.* **9**, 745 (2018).
9. Nauta, T. D. et al. Hypoxic signaling during tissue repair and regenerative medicine. *Int. J. Mol. Sci.* **15**, 19791–19815 (2014).
10. Ott, C. et al. SIPS as a model to study age-related changes in proteolysis and aggregate formation. *Mech. Ageing Dev.* **170**, 72–81 (2018).
11. Vono, R. et al. Oxidative stress in mesenchymal stem cell senescence: regulation by coding and noncoding RNAs. *Antioxid. Redox Signal* **29**, 864–879 (2018).
12. Barshes, N. R., Wyllie, S. & Goss, J. A. Inflammation-mediated dysfunction and apoptosis in pancreatic islet transplantation: implications for intrahepatic grafts. *J. Leukoc. Biol.* **77**, 587–597 (2005).
13. Cappelli, A. P. G. et al. Reduced glucose-induced insulin secretion in low-protein-fed rats is associated with altered pancreatic islets redox status. *J. Cell. Physiol.* **233**, 486–496 (2018).
14. Tejchman, K., Kotfis, K. & Sieńko, J. Biomarkers and mechanisms of oxidative stress-last 20 years of research with an emphasis on kidney damage and renal transplantation. *Int. J. Mol. Sci.* **22**, 8010 (2021).
15. Farina, M. et al. Cell encapsulation: overcoming barriers in cell transplantation in diabetes and beyond. *Adv. Drug. Deliv. Rev.* **139**, 92–115 (2019).
16. Yao, Q. et al. Localized controlled release of bilirubin from β-cyclodextrin-conjugated ε-polylysine to attenuate oxidative stress and inflammation in transplanted islets. *Acs. Appl. Mater. Interfaces* **12**, 5462–5475 (2020).
17. Zhang, Y. et al. The dual effects of reactive oxygen species on the mandibular alveolar bone formation in SOD1 knockout mice: promotion or inhibition. *Oxid. Med. Cell. Longev.* **2021**, 8847140 (2021).
18. Evans, R. M. & Mangelsdorf, D. J. Nuclear receptors, rxr, and the big bang. *Cell* **157**, 255–266 (2014).
19. Lu, M. et al. Brain PPAR-γ promotes obesity and is required for the insulin-sensitizing effect of thiazolidinediones. *Nat. Med.* **17**, 618–622 (2021).
20. Stienstra, R. et al. Peroxisome proliferator-activated receptor gamma activation promotes infiltration of alternatively activated macrophages into adipose tissue. *J. Biol. Chem.* **283**, 22620–22627 (2008).
21. Charo, I. F. Macrophage polarization and insulin resistance: ppar gamma in control. *Cell. Metab.* **6**, 96–98 (2007).
22. Elshazly, S. & Soliman, E. PPAR gamma agonist, pioglitazone, rescues liver damage induced by renal ischemia/reperfusion injury. *Toxicol. Appl. Pharm.* **362**, 86–94 (2019).
23. Li, H. et al. Recruited CD68+CD206+ macrophages orchestrate graft immune tolerance to prompt xenogeneic-dentin matrix-based tooth root regeneration. *Bioact. Mater.* **6**, 1051–1072 (2020).
24. Yang, B. et al. Tooth root regeneration using dental follicle cell sheets in combination with a dentin matrix - based scaffold. *Biomaterials* **33**, 2449–2461 (2012).
25. Li, H. et al. Xenogeneic bio-root prompts the constructive process characterized by macrophage phenotype polarization in rodents and nonhuman Primates. *Adv. Healthc. Mater.* **6**, 1601112 (2017).
26. Li, R. et al. Human treated dentin matrix as a natural scaffold for complete human dentin tissue regeneration. *Biomaterial* **32**, 4525–4538 (2011).
27. Han, X. et al. Xenogeneic native decellularized matrix carrying PPARγ activator RSG regulating macrophage polarization to promote ligament-to-bone regeneration. *Mater. Sci. Eng. C: Mater. Biol. Appl.* **116**, 111224 (2020).
28. Saito, K. et al. Dentin Matrix Protein 1 Compensates for lack of osteopontin in regulating odontoblastlike cell differentiation after tooth injury in mice. *J. Endod.* **46**, 89–96 (2020).
29. Xia, L. et al. CHD4 has oncogenic functions in initiating and maintaining epigenetic suppression of multiple tumor suppressor genes. *Cancer Cell* **31**, 653–668.e7 (2017).
30. Lai, L. et al. Type 5 adenylyl cyclase increases oxidative stress by transcriptional regulation of manganese superoxide dismutase via the SIRT1/FoxO3a pathway. *Circulation* **127**, 1692–1701 (2013).
31. Sinem, F. et al. The serum protein and lipid oxidation marker levels in Alzheimer's disease and effects of cholinesterase inhibitors and antipsychotic drugs therapy. *Curr. Alzheimer Res.* **7**, 463–469 (2010).
32. Kyogoku, Y. et al. Nitrosative stress in patients with asthma-chronic obstructive pulmonary disease overlap. *J. Allergy Clin. Immunol.* **144**, 972–983.e14 (2019).
33. Rangwala, S. M. & Lazar, M. A. Peroxisome proliferator-activated receptor gamma in diabetes and metabolism. *Trends Pharmacol. Sci.* **25**, 331–336 (2004).
34. Rosen, E. D. et al. PPAR gamma is required for the differentiation of adipose tissue in vivo and in vitro. *Mol. Cell* **4**, 611–617 (1999).
35. Deng, J. et al. Protective effect of rosiglitazone on chronic renal allograft dysfunction in rats. *Transpl. Immunol.* **54**, 20–28 (2019).
36. Silveira, L. S. et al. Exercise rescues the immune response fine-tuned impaired by peroxisome proliferator-activated receptors γ deletion in macrophages. *J. Cell. Physiol.* **234**, 5241–5251 (2019).
37. Kotha, S. et al. An in-silico approach: identification of PPAR-γ agonists from seaweeds for the management of Alzheimer's Disease. *J. Biomol. Struct. Dyn.* **39**, 2210–2229 (2021).
38. Lee, Y. et al. Neuroprotective effects of MHY908, a PPAR α/γ dual agonist, in a MPTP-induced Parkinson's disease model. *Brain. Res.* **1704**, 47–58 (2019).
39. Janani, C. & Ranjitha Kumari, B. D. PPAR gamma gene–a review. *Diabetes Metab. Syndr.* **9**, 46–50 (2015).
40. Spriano, S. et al. A critical review of multifunctional titanium surfaces: New frontiers for improving osseointegration and host response, avoiding bacteria contamination. *Acta Biomater.* **79**, 1–22 (2018).
41. Gholipourmalekabadi, M. et al. In vitro and in vivo evaluations of three-dimensional hydroxyapatite/silk fibroin nanocomposite scaffolds. *Biotechnol. Appl. Biochem.* **62**, 441–450 (2015).
42. Jin, S. S. et al. A biomimetic hierarchical nanointerface orchestrates macrophage polarization and mesenchymal stem cell recruitment to promote endogenous bone regeneration. *Acs. Nano* **13**, 6581–6595 (2019).
43. Kwiatkowska, M. et al. Potential effects of immunosuppression on oxidative stress and atherosclerosis in kidney transplant recipients. *Oxid. Med. Cell. Longev.* **2021**, 6660846 (2015).
44. Colombo, G. et al. Plasma protein carbonyls as biomarkers of oxidative stress in chronic kidney disease, dialysis, and transplantation. *Oxid. Med. Cell. Longev.* **2020**, 2975256 (2020).
45. Wang, Z. et al. Effect of ozone oxidative preconditioning on inflammation and oxidative stress injury in rat model of renal transplantation. *Acta Cir. Bras.* **33**, 238–249 (2018).
46. Kargin, R. et al. Role of the oxidative stress index, myeloperoxidase, catalase activity for cardiac allograft vasculopathy in heart transplant recipients. *Clin. Transpl.* **32**, e13273 (2018).
47. Schimke, I. et al. Oxidative stress in the human heart is associated with changes in the antioxidative defense as shown after heart transplantation. *Mol. Cell. Biochem* **204**, 89–96 (2000).
48. Szczurek, W. et al. Investigation of the role of oxidative stress and factors associated with cardiac allograft vasculopathy in patients after heart transplantation. *Oxid. Med. Cell. Longev.* **2020**, 7436982 (2020).
49. Banci, L. et al. Atomic-resolution monitoring of protein maturation in live human cells by NMR. *Nat. Chem. Biol.* **9**, 297–299 (2013).
50. Pouyet, L. & Carrier, A. Mutant mouse models of oxidative stress. *Transgenic. Res.* **19**, 155–164 (2010).
51. Jaarsma, D. et al. CuZn superoxide dismutase (SOD1) accumulates in vacuolated mitochondria in transgenic mice expressing amyotrophic lateral sclerosis-linked SOD1 mutations. *Acta Neuropathol.* **102**, 293–305 (2001).

52. Hashizume, K. et al. Retinal dysfunction and progressive retinal cell death in SOD1-deficient mice. *Am. J. Pathol.* **172**, 1325–1331 (2008).
53. Hang, Y. et al. CuZnSOD gene deletion targeted to skeletal muscle leads to loss of contractile force but does not cause muscle atrophy in adult mice. *FASEB. J.* **27**, 3536–3548 (2013).

Open Access This article is licensed under a Creative Commons Attribution 4.0 International License, which permits use, sharing, adaptation, distribution and reproduction in any medium or format, as long as you give appropriate credit to the original author(s) and the source, provide a link to the Creative Commons license, and indicate if changes were made. The images or other third party material in this article are included in the article's Creative Commons license, unless indicated otherwise in a credit line to the material. If material is not included in the article's Creative Commons license and your intended use is not permitted by statutory regulation or exceeds the permitted use, you will need to obtain permission directly from the copyright holder. To view a copy of this license, visit http://creativecommons.org/licenses/by/4.0/.

© The Author(s) 2023